SINGLE ELECTRON DYNAMIC OF MICROWAVE UNDULATOR

C. Chang, J. Neilson, C. Pellegrini, M. Shumail, S. Tantawi,
SLAC National Accelerator Laboratory, Stanford University, Stanford, CA 94309, USA

Abstract

The analytical and numerical calculations for the dynamic of single electron and beam in RF undulator have been conducted and compared. The transverse and longitudinal velocity, trajectory, energy variation, and the spontaneous radiation are studied. It is found that the forward and backward wave (FW/BW) components have different contribution on electron motion and radiation, most of the energy spread comes from FW component, in other words, the effect of FW on modulating the electron energy is much stronger than that of BW for the same undulating-amplitude value, which mechanism has been analyzed.

INTRODUCTION

Compared to conventional static magnetic undulators,[1] RF undulators have obvious advantages[2-6] in variable polarization of spontaneous radiation, and weak influence of wakefield due to large aperture. The electron dynamics of an RF undulator have special character due to the complex electric-magnetic modes; the HE_{11} mode, which has a low loss on walls, is selected, and the dynamic is researched both analytically and numerically.

DYNAMICS FOR RF UNDULATOR

HE_{11} Mode in the Corrugated Waveguide

The structure of the corrugated waveguide is shown in Fig.1(a).

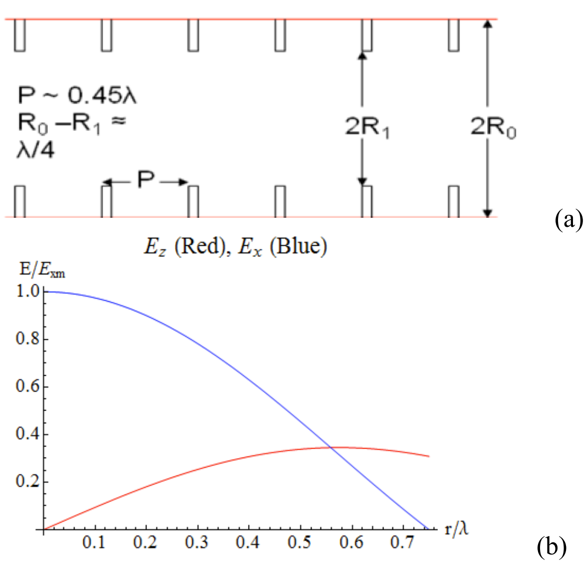

Figure 1: (a) Corrugated waveguide structure and (b) E_x and E_z field distribution with radius r (R_0=λ).

Adopting a Cartesian coordinate system, where the z-axis coincides with the undulator axis, the transverse electric field E_x of HE_{11} mode satisfies a perfect linearly polarization and has a similarly radial distribution of the Bessel function $J_0(k_r r)$ shown in Fig.1(b), which produces the main wiggling motion in the RF undulator; the longitudinal electric field E_z with $J_1(k_r r)$, shown in Fig.1(b), has a weak impact on the beam near the axis and with radius $r_m \sim (\beta_\varepsilon \varepsilon)^{0.5} \sim 1$mm. The radius of the corrugated waveguide chooses $R_0 \sim \lambda$, the wavelength in free space, to decrease the total loss to minimum for HE_{11} mode.

Single Electron Dynamic

The simplified normalized vector potentials for the HE_{11} mode are written as:

$$A_x = K J_0(k_r r)\sin(\omega t \pm k_z z + \varphi) \tag{1}$$

$$A_z = K(k_r/k_z) J_1(k_r r)\cos(\omega t \pm k_z z + \varphi)\, x/r \tag{2}$$

where J_0 and J_1 Bessel functions, $r=(x^2+y^2)^{0.5}$, the dispersion relation $k_r^2+k_z^2=k^2$, $k_r=2.405/R_1$[7], $R_1=0.75R_0$, the waveguide radius $R_0=\lambda$, "$-k_z z$" for FW, "$+k_z z$" for BW, and φ is the RF phase. For a standing wave,

$$A_x = 2K_0 J_0(k_r r)\sin(\omega t+\varphi)\cos(k_z z) \tag{3}$$

$$A_z = 2K_0 (k_r/k_z) J_1(k_r r)\cos(\omega t+\varphi)\cos(k_z z)\, x/r \tag{4}$$

The normalized electric and magnetic field component of the electromagnetic wave can be solved by,

$$\boldsymbol{E} = -\partial \boldsymbol{A}/\partial t \quad \text{and} \quad \boldsymbol{B} = \nabla \times \boldsymbol{A} \tag{5}$$

The dimensionless Hamiltonian equation for relativistic electrons reads,

$$\boldsymbol{H} = \sqrt{(\boldsymbol{P}-\boldsymbol{A})^2 + 1} \tag{6}$$

where the normalized canonical momentum $\boldsymbol{P}$ and Hamiltonian H have been respectively normalized by mc and mc^2. The mechanical momentum satisfies $\boldsymbol{p}=\boldsymbol{P}-\boldsymbol{A}$. Since the relativistic electron satisfies γ >>1, the space charge field can be neglected, its motion is mainly determined by the field of the undulator. By solving the Hamiltonian equation and the six first-order differential equations $\dot{x} = \partial H/\partial P_x$, $\dot{y} = \partial H/\partial P_y$, $\dot{z} = \partial H/\partial P_z$, $\dot{p}_x = -\partial H/\partial x$, $\dot{p}_y = -\partial H/\partial y$, and $\dot{p}_z = -\partial H/\partial z$. The trajectory and energy of a single electron can be obtained by numerical calculation. The adopted parameters are B_{ym}=0.4 T for travelling wave, f=11.424 GHz, $K=(eB_{ym}/m\omega)=0.9807$,

ISBN 978-3-95450-115-1

initial electron coordinate x_0=0.038λ, y_0=0, and z_0=0, initial momentum p_x=0 and p_y=0, electron energy ε_e=60 MeV, and undulator length L=1 m corresponding to 38.18λ. By numerically calculating the Hamiltonian equations, the trajectory and energy of a single electron for FW, BW and SW are shown in Fig. 2.

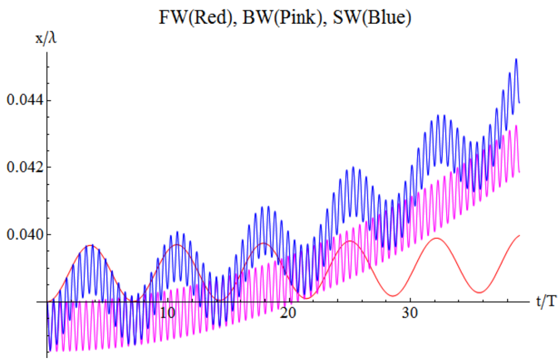

Figure 2: Transverse trajectory of single electron for FW, BW and SW (φ=0°).

The numerical results shown in Fig. 2 reveal that, for FW, the motion of an electron has a low oscillation frequency ~$(1-k_z/k)f$,. For BW the oscillation frequency is high, ~$(1+k_z/k)f$. Thus, the trajectory under SW contains multiple frequencies.

For electron beam near the waveguide axis, with beam radius r_m~1 mm=0.038λ<< R_0~λ for f=11.424 GHz, the Bessel function in the vector potential of Eq. (1) and (2) can be approximately expanded into a Taylor series up to the second order; thus, $J_0(k_r r)=1-k_r^2r^2/4$, $J_1(k_r r)=k_r r/2-(k_r r)^3/8$, and the dimensionless undulator field is $K=(eB_{ym}/m\omega)(1-k_r^2r^2/4)$. The beam radius r_m~0.038λ, $k_r^2r_m^2/4\approx0.004$, $r_m k_r^2/k_z=0.07$; thus, $|A_z|<<|A_x|$ for electrons close to the axis. Besides, when R_0 increases, k_r becomes small; thus, the transverse field becomes relative uniform. It is reasonable to take a constant K and neglect A_z as a first step, and the oscillation of longitudinal motion is determined by the transverse wiggling motion. The normalized longitudinal velocity for BW approximately can be derived as

$$\beta_{zB}=\sqrt{1-\beta_{xB}^2-1/\gamma^2}\approx\left\{1-\frac{1+K^2/2}{2\gamma^2}+\frac{K^2\cos\left(2\left(k+k_z\right)z\right)}{4\gamma^2}\right\} \tag{7}$$

The initial longitudinal velocity is $\beta_{z0}=(1-\gamma^{-2})^{0.5}$, thus $\Delta\beta_{zB}=\beta_{zB}-\beta_{z0}$, similarly, the normalized longitudinal velocity for FW approximately yields,

$$\beta_{zF}\approx\left\{1-\frac{1+K^2/2}{2\gamma^2}+\frac{K^2\cos\left(2\left(k-k_z\right)z\right)}{4\gamma^2}\right\} \tag{8}$$

The normalized longitudinal velocity for SW approximately can be derived as,

$$\beta_{zS}=\sqrt{1-\beta_x^2-1/\gamma^2}\approx\left\{\begin{array}{l}1-\dfrac{1+K^2}{2\gamma^2}-\dfrac{K^2\left(-\cos\left(2kz\right)+\cos\left(2k_z z\right)\right)}{2\gamma^2}\\ -K^2\left(\cos\left(2\left(k+k_z\right)z\right)+\cos\left(2\left(k-k_z\right)z\right)\right)/\left(4\gamma^2\right)\end{array}\right\} \tag{9}$$

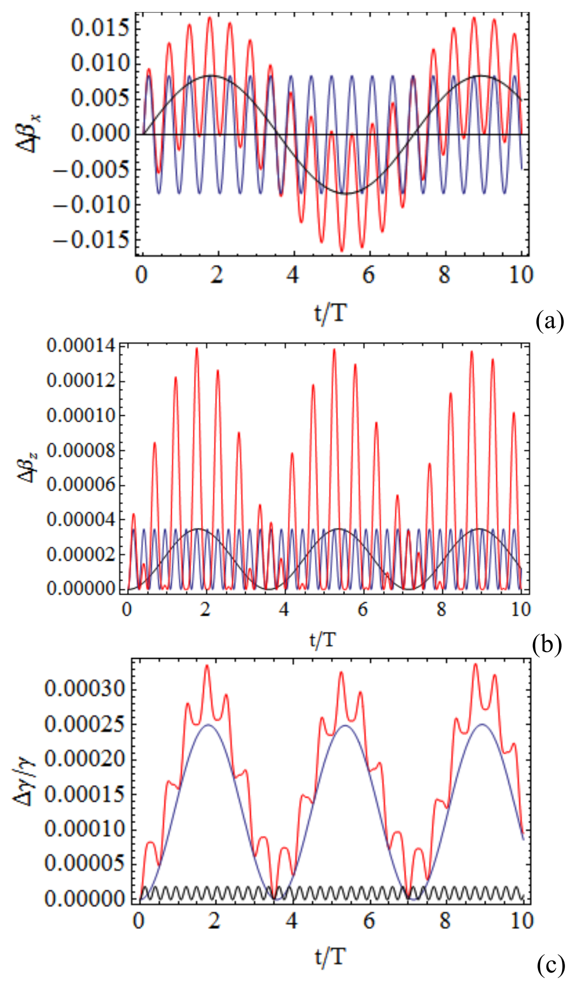

Figure 3: Comparison of numerical (a) $\Delta\beta_x$, (b) $\Delta\beta_z$, and (c) Δγ/γ for BW (*blue*), FW (*black*), and SW (*red*) with Az=0. (K=1, γ=117.4).

If A_z=0, electrons at different transverse positions, from the axis to x_m=±0.038λ, have the same amplitude of $\Delta\beta_x$, $\Delta\beta_z$ and Δγ/γ no matter for BW, FW, or SW, since $J_0(k_r r)=1-k_r^2r^2/4$ changes little. Comparisons of numerical $\Delta\beta_x$, $\Delta\beta_z$, and Δγ/γ for BW, FW, and SW are shown in Fig. 3. It is found that the analytical values of $\Delta\beta_z$ for BW, FW, and SW from Eqs. (7-9) are perfectly consistent with the numerical ones in Fig. 3(b). Note that the longitudinal motion contains four harmonic oscillations for SW. The energy spread Δγ/γ for SW mainly arises from FW and reaches about 0.03% for ε_e=60 MeV.

After considering A_z, electrons at different transverse positions have significantly different amplitudes of $\Delta\gamma$, which increases to 0.4% at $x_m=\pm$ 0.038λ (~ ±1 mm), significantly larger than that on the axis, since $A_z \sim J_1(k_r r)$ quickly increases. $\Delta\gamma/\gamma$ for SW mainly arises from the influence of A_z of FW, shown in Fig. 4. Decreasing the beam size in both transverse directions has a better effect on diminishing energy spread in an RF undulator.

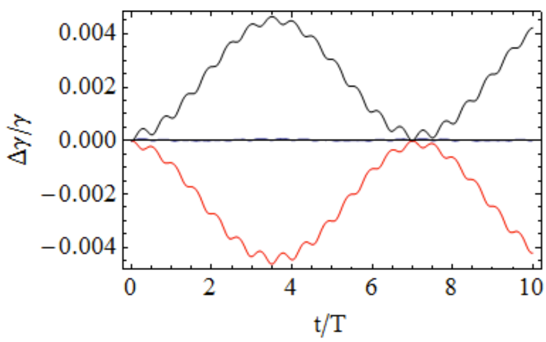

Figure 4. Variation of $\Delta\gamma/\gamma$ for SW with Az, where x=0 (*blue*), $x=x_m\sim0.038\lambda$ (*black*), $x=-x_m$ (*red*) (K=1, γ=117.4).

CONCLUSION

The forward and backward wave (FW/BW) components have different contributions to electron motion and radiation. For FW, the motion of election has a low oscillation frequency $\sim(1-k_z/k)f$, As a comparison, for BW, a high oscillation frequency $\sim(1+k_z/k)f$. Thus, trajectory under SW contains multiple frequencies. Most of the energy spread comes from the FW component; the effect of FW on modulating the electron energy is much stronger than that of BW for the same undulating-amplitude value.

REFERENCES

[1] Shea, F., Marcus, G. Rosenzweig, J. B., Scheer, M. Bahrdt, J., Weingartner, R., Gaupp, A. Gruner, F., "Short Period, High Field Cryogenic Undulator for Extreme Performance X-ray Free Electron Lasers," Phys. Rev. ST Accel. Beams **13** (2010) 070702.

[2] S. Tantawi, V. Dolgashev, C. Nantista, C. Pellegrini, J. Rosenzweig, G. Travish, "A Coherent Compton Backscattering High Gain FEL using an X-Band Microwave Undulator," 2005 FEL Conference, Stanford, California, USA; http://accelconf.web.cern.ch/accelconf/f05/PAPERS/THOA006.PDF

[3] T. Shintake, K. Huke, J. Tanaka, I. Sato and I. Kumabe, "Development of microwave undulator", Japanese J. of Appl. Phys. **22** (1983), p. 844-851.

[4] T.M. Tran, B.G. Danly, J.S. Wurtele, "Free-Electron Lasers with Electromagnetic Standing Wave Wigglers", IEEE J. Quantum Electronics **QE-23** (1987), pp. 1578-1589.

[5] M. Yeddulla, H. Geng, Z. Ma, Z. Huang, S. Tantawi, "Waveguide Structures for RF Undulators with Applications to FELs and Storage Rings," Proceedings of EPAC08, Genoa, Italy; http://accelconf.web.cern.ch/accelconf/e08/papers/wepc136.pdf

[6] C. Pellegrini, "X-Band Microwave Undulators for Short Wavelength Free-Electron Lasers," 2005 FEL Conference 2005, Stanford, California, USA; http://accelconf.web.cern.ch/accelconf/f05/PAPERS/MOPP060.PDF

[7] P.J.B. Clarricoats and A.D. Olver, *Corrugated horns for microwave antennas*, Peter Peregrinus Ltd, London, UK, 1984.

ISBN 978-3-95450-115-1